Laboratory testing of coupled hydro-mechanical processes during rock deformation

Juliane Heiland

Abstract This paper gives an overview of the published literature on laboratory testing of the stress dependence of rock-permeability. Additionally results of personal research on the stress dependence of the permeability of a low-porosity sandstone are presented. Stress-dependent permeability is examined in the laboratory under different stress fields and stress paths, depending on the intended application of the research. The most commonly applied stress paths are hydrostatic compression, triaxial compression, uniaxial strain conditions, and testing under a constant stress path. The published results of several studies on different rock types under one or more of the mentioned stress conditions are described and compared.

A general trend of permeability evolution under hydrostatic and triaxial conditions can be established for sandstones and some crystalline rocks such as granite or rocksalt. For uniaxial strain tests and stress path tests the published results are limited to a few rock types (mainly sandstones). Therefore, a general conclusion for the stress dependence of permeability under these conditions is not possible.

Résumé Cet article donne une vue d'ensemble de la littérature publiée sur les essais de laboratoire concernant la dépendance de la perméabilité de la roche à la contrainte. En plus, les résultats d'une étude sont présentés sur la dépendance de la perméabilité d'un grès à faible porosité à la contrainte. La perméabilité sous contrainte est analysée au laboratoire sous différents champs et différents types de contraintes, en fonction des applications des recherches. Les types de contraintes les plus couramment appliqués sont la compression hydrostatique, la compression triaxiale, la condition de contrainte uniaxiale et l'essai sous une contrainte constante. Les résultats publiés par plusieurs auteurs examinant des types de roches différents sous une ou plusieurs conditions de contrainte mentionnées sont décrits et comparés. Une tendance générale de l'évolution de la perméabilité sous des conditions hydrostatique et triaxiale peut être établie pour les roches poreuses (par exemple des grès) et certaines roches cristallines (par exemple le granite, ou les roches salines). Pour les essais sous contrainte uniaxiale et les types de contraintes les résultats publiés sont limités à quelques types de roches (surtout des grès). C'est pourquoi une conclusion plus générale sur la dépendance de la perméabilité de la roche à la contrainte n'est pas possible dans ces conditions.

Resumen El presente artículo ofrece una visión general de los trabajos publicados sobre ensayos de laboratorio que hayan investigado la dependencia de la permeabilidad de la roca con la tensión, añadiendo resultados de cosecha propia en relación con areniscas de baja permeabilidad. Se examina la dependencia de la permeabilidad con la tensión en laboratorio bajo diferentes campos y direcciones de los esfuerzos, en función de la aplicación pretendida por el estudio. Las direcciones de tensión aplicadas más a menudo son la compresión hidrostática, la compresión triaxial, la condición de deformación uniaxial y la testificación bajo dirección de tensión constante. Se describe y compara los resultados publicados por varios autores en diferentes tipos de roca, de acuerdo con una o más de la condiciones citadas. Se puede establecer una tendencia general de la evolución de la permeabilidad bajo condiciones hidrostáticas y triaxiales para rocas porosas (por ejemplo, areniscas) y para algunas rocas cristalinas (como granitos o sal). En el caso de ensayos de deformación y de direcciones de tensión uniaxiales, los resultados publicados se limitan a unos pocos tipos de roca, principalmente areniscas. Por tanto, no es posible llegar a una conclusión más genérica sobre la dependencia de la permeabilidad con la tensión en dichas condiciones.

J. Heiland (✉)
Schlumberger Cambridge Research,
High Cross, Madingley Road, Cambridge, CB3 0EL UK
e-mail: jheiland@cambridge.oilfield.slb.com
Tel.: +44-1223-325259, Fax: +44-1223-327019

Introduction

Permeability of rocks is widely assumed to be a rock property, but a study of the stress state of the sample and its effect on permeability reveals it is more a 'process'

than a 'material' property because it changes within one formation due to changed boundary conditions (e.g. stress, deformation).

This paper reviews published research concerning the stress sensitivity of the matrix permeability of rocks. The focus is on experimental studies in the laboratory scale. These studies mostly investigated arenitic rocks (sandstones), crystalline rocks and rocksalt. Additionally, results are presented from personal experimental work on the permeability evolution of a low-porosity sandstone undergoing triaxial compression.

Discussion

The permeability of rocks was exhaustedly studied under hydrostatic stress conditions (e.g. Zoback and Byerlee 1975a; Walsh and Brace 1984; Morrow et al. 1984; David et al. 1994) in order to establish effective pressure laws for the permeability of different rock types. However, in the field, rocks are normally subjected to a non-homogenous stress-field where the vertical stress (determined by the weight of the overburden) is exceeding the two horizontal stresses (Holt 1990). An increasing number of studies has been published in the last years concerning the sensitivity to non-hydrostatic stress conditions of the matrix permeability of arenitic rocks. Most of these studies incorporated the analysis of several possible stress conditions, the most common ones being hydrostatic compression, triaxial compression and uniaxial strain condition. Some studies investigated the influence of different stress paths on permeability.

All studies used cylindrical samples with the longer axis subjected to the axial stress, which normally corresponds to the maximum (normally vertical) stress in the field. Unless otherwise noted, the permeability was measured along the sample axis, that is, parallel to the maximum stress direction.

Depending on the application of the research, different rock types were investigated. The petroleum industry is mainly interested in the properties of arenitic rocks, and investigations for underground waste repositories are mainly concentrated on rocksalt, clayey rocks and crystalline rocks.

For underground waste disposal in general the permeability of the rock mass surrounding the repository should be as small as possible. This means that research in this field is focused on the enhancement of permeability within an excavation-disturbed-zone (EDZ). In very brittle rocks (such as crystalline rocks), the EDZ results in increased fracture permeability, which is not dealt with in this paper. In ductile rocks, such as rocksalt, the research is focused on the onset of dilatant rock behaviour under increasing stress and the accompanying permeability increase. This is normally investigated using creep tests or standard triaxial tests.

The permeability of a rock formation is of great interest to the oil industry because it may control reservoir productivity. During the depletion of an oil reservoir, the pore pressure normally decreases, which results in increasing effective vertical and horizontal stresses. This can cause compaction, which, in turn, can impact matrix permeability. Usually, it is assumed that during reservoir depletion the rock mass is subjected to uniaxial strain conditions, which means that only vertical compaction occurs due to increasing effective vertical stresses and that lateral deformation is zero (Schutjens et al. 1997). However, stress measurements have shown that a reservoir can undergo different stress paths, depending on the boundary conditions, geometry and poro-elastic properties of the rock mass.

Stress path is sometimes denoted K and is defined as the "constant ratio of change in effective minimum (horizontal) stress to effective maximum (vertical) stress from initial reservoir conditions" (Ruisten et al. 1999). To distinguish stress path from permeability, which is also commonly abbreviated with K, the stress path will be denoted with K and permeability with k.

$$K = \Delta\sigma_{min} / \Delta\sigma_{max} \qquad (1)$$

With K=stress path, σ_{min}=minimum (horizontal) stress and σ_{max}=maximum (vertical) stress.

Hydrostatic compression represents a stress path of K=1 and laboratory experiments under uniaxial strain conditions are usually denoted K_0-tests and are meant to determine the uniaxial compressibility of a rock, which is assumed to be a rock property.

Testing Concepts of Rock Mechanics

In the laboratory, the influence of various stress conditions on matrix permeability can be investigated using different types of experiments. Hydrostatic compression tests determine the influence of increasing effective pressure on permeability. For this, all principle stresses (σ_1, σ_2 and σ_3) are assumed to be equal and the effective pressure is calculated from:

$$\sigma_{eff} = \sigma_3 - \sigma_{fl} \qquad (2)$$

with σ_{eff} effective pressure, σ_3 hydrostatic pressure and σ_{fl} pore fluid pressure.

The typical time development of the pressures acting in and around a cylindrical sample during a hydrostatic compression test is shown in Fig. 1A. Figure 1B shows this for a triaxial compression test, in which a cylindrical rock sample is subjected to a confining pressure (σ_3), which is acting on the cylinder wall and is kept constant during the whole experiment. This means that both horizontal stresses are assumed to be equal ($\sigma_2=\sigma_3$). In axial direction the stress (σ_1) is increased during the experiment, until failure of the sample occurs. The axial stress is normally increased in strain control, subjecting the sample to a constant deformation rate, which enables the continuation of the experiment into the post-failure region. When permeability is determined during these experiments, a pore pressure is applied, which is also kept constant during the whole experiment.

A third kind of laboratory test are stress path experiments, where σ_1 and σ_3 are following a stress path

Fig. 1A–C Schematic time development and schematic view of pressure and stress acting on the experimental specimens. **A** Hydrostatic compression, **B** triaxial compression, **C** uniaxial strain test
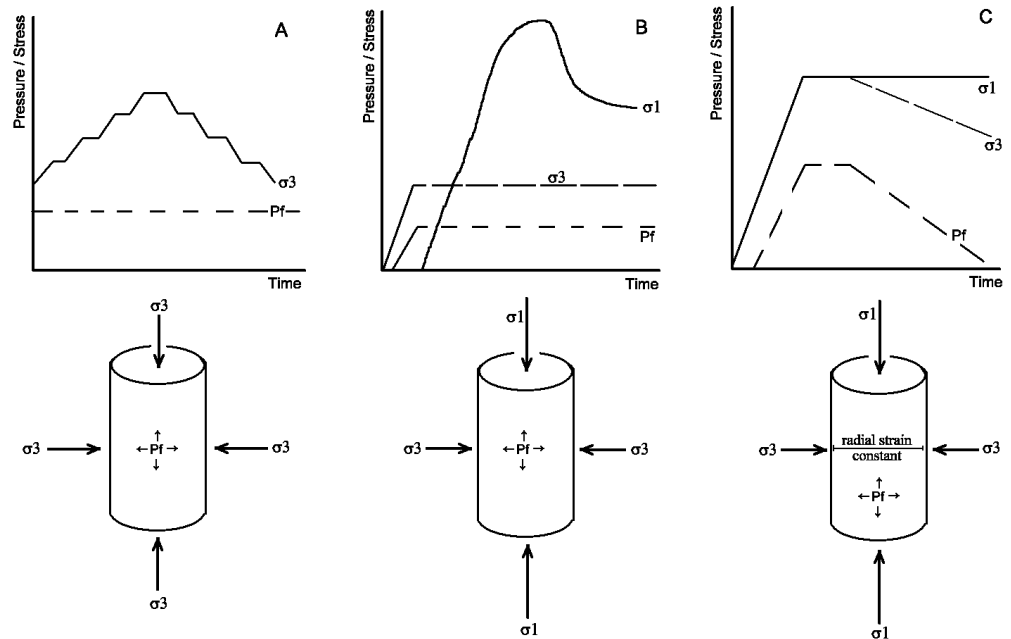
K between 1 (hydrostatic compression) and 0 (constant stress boundary). A special type of stress experiment is the uniaxial strain test (see Fig. 1C), where starting at hydrostatic conditions the axial stress is kept constant, pore pressure is linearly decreased and the lateral strain is kept constant by adjusting the confining pressure.

Very specialized laboratory experiments are true triaxial tests and triaxial extension tests. The latter ones are used for (indirectly) measuring the tensile strength of rock. For this, the rocks are hydrostatically compressed to a high initial pressure. The axial stress is then lowered until the sample fails by forming a horizontal fracture. In true triaxial tests all three principle stresses are controlled separately.

Relevance of the testing procedures
for field applications
Stress-path experiments and uniaxial strain tests are mainly used in the petroleum industry to simulate and investigate the depletion of an oil reservoir. Hydrostatic compression tests are relatively simple to perform in the laboratory and, thus, are the most common way for investigating the stress sensitivity of a porous rock. However, in nature, this kind of stress path is not commonly found.

Triaxial compression tests are mainly used to determine the failure criterion of a rock. It is a standard test frequently performed in every rock mechanics laboratory, although it is not directly resembling any field situation. In true triaxial tests the real stress conditions of a field situation can be directly simulated. Triaxial extension tests are an indirect way of determining the tensile strength of rock.

Permeability Measurement

During all these experiments, permeability can be measured either by using steady-state flow or a transient pulse method. Both methods have been described in many publications and textbooks, for more details see, for example, Kranz et al. (1990), Brace et al. (1968) and Walsh and Brace (1984).

The measurement of permeability is generally linked to Darcy's law, which describes the connection between flow rate, fluid pressure, geometry of the flow path and properties of the flowing fluids as well as properties of the porous medium.

Darcy's law is written as:

$$q = k \cdot A \frac{\Delta h}{L} \tag{3}$$

with *q* flow rate (m³/s), *k* coefficient of permeability (m/s) or hydraulic conductivity, *A* cross-sectional area of flow (m²), Δh hydraulic head (m) and *L* length of flow path (m).

A shortened version of this equation is:

$$q = k \cdot i \cdot A \tag{4}$$

with *i* hydraulic gradient ($i = -\dfrac{dh}{dx}$).

From these equations it follows that *k* is assumed to be a constant, which depends on the fluid properties as well as on the rock properties. When using the 'intrinsic permeability', here just called permeability, Darcy's law can be written as:

$$q = -k \frac{\gamma_f}{\mu} \cdot \frac{dh}{dx} \cdot A \tag{5}$$

with *k* (intrinsic) permeability (m²), γ_f unit weight of fluid (water: 1,000 kg/m³) and μ viscosity of fluid (water at 20 °C: 10⁻³ Pa s⁻¹).

Using the steady-state method, a constant fluid flow between pore fluid inlet and outlet (typically located at the upper and lower ends of a cylindrical sample, so that the flow direction is parallel to σ_1) is established by either keeping the flow rates constant and equal at both ends of the sample and measuring the pressure difference, or setting up a specified pressure difference and measuring the resulting flow rates. When using the steady-state method for permeability measurement, Eq. (5) can be re-written so that the permeability can be calculated from the measured pressure differences and flow rates:

$$k = \frac{q \cdot \mu \cdot L}{A \cdot \Delta P} \tag{6}$$

with q flow rate, L sample length, μ viscosity of the fluid, ΔP pressure difference across sample length and A is the sample area.

When measuring permeability using a steady-state method, the boundary conditions such as stress and deformation should also be kept constant, assuring that the conditions for which Darcy's law is valid are met. During triaxial tests, this is normally achieved by stopping the movement of the axial actuator. However, at high differential stresses close to rock failure, locking the actuator does not always stop sample deformation because of stress relaxation and ongoing deformation (creep in lateral and axial direction).

For the transient pulse method a constant pore pressure is maintained in the sample and adjacent upper and lower fluid reservoir. For a measurement, the pressure in the upper reservoir is instantaneously increased by a small amount and the pressure decay at both reservoirs is monitored. Permeability is then determined from the pressure decay vs. time plots (Brace et al. 1968; Keaney et al. 1998). The time needed for the pressure decay varies according to the permeability and can be up to several hours (Brace et al. 1968). The transient method requires that permeability is constant during the whole measurement time. Keaney et al. (1998) addressed this by reducing the load following a standardized procedure, trying to get stable stress/strain conditions during the permeability measurement.

Another transient permeability measurement technique was described by Kranz et al. (1990) who used an oscillating pore pressure method to calculate permeability and diffusivity under variable external conditions. A saturated cylindrical rock sample was used, which was connected to an upstream and downstream fluid reservoir with the whole system brought to an elevated pore pressure level. Then a constant oscillating pore pressure signal was applied to the downstream reservoir and the output of this signal was measured at the downstream reservoir. From the time shift and the amplitude decay of the signal, permeability and diffusivity were calculated. The frequency of the upstream signal had to be adjusted according to the intrinsic hydraulic properties of the rock sample.
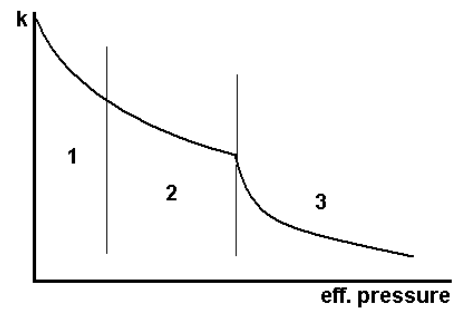

Fig. 2 Schematic plot of permeability k vs. effective pressure (σ_{eff}) for hydrostatic compression, showing three phases of hydrostatic compaction: *1* microcrack closure, *2* exponential permeability reduction due to pore compaction and relative grain movement and *3* grain crushing. *k* Permeability (after David et al. 1994; Keaney et al. 1998)

Experiments Investigating Stress Sensitivity of Rock Permeability

The following sections give an overview of publications describing experimental work on the stress sensitivity of different rock types. The published results are commented on based on the results of personal research. This analysis is structured according to the types of experiments described and conclusions are given for individual groups of experiments. It starts with experiments that can be grouped as stress path experiments in the wider sense, i.e. hydrostatic compression, specific stress paths and uniaxial strain tests. The second group of experiments are triaxial compression, triaxial extension and true triaxial tests.

Group A: Stress Path Experiments (in a Wider Sense)
Hydrostatic compression
In general, under hydrostatic compression, the matrix permeability of rocks decreases with increasing effective stress. Three phases of compactional behaviour can be distinguished (Fig. 2).

1. A high reduction rate at low effective pressure, which is probably due to microcrack closure (David et al. 1994).
2. The rate of permeability reduction decreases at higher effective pressures, and is then followed by an approximately exponential decay (David et al. 1994). Keaney et al. (1998) show that not only permeability, but also the specific storage (i.e. the amount of water stored in the pore volume), decreases with increasing effective pressure. While permeability decreases by one order of magnitude, storage decreases by only a factor of two. This is explained by the assumption that the closure of microcracks is volumetrically not very significant, but the closure of fluid pathways affects permeability very much.
3. When the effective pressure is increased further, porous rocks exhibit a sharp decline in permeability, which indicates the onset of non-elastic deformation,
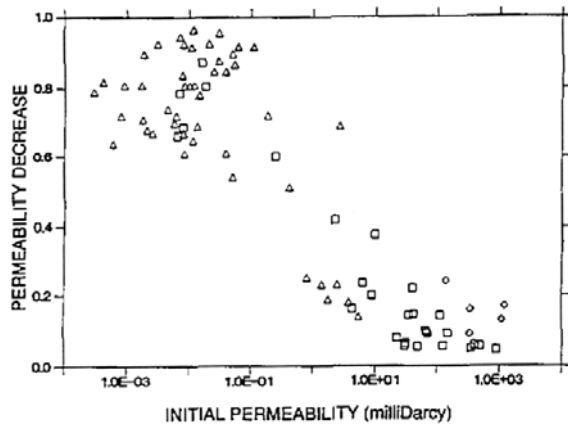
Fig. 3 Permeability change during hydrostatic compression plotted vs. initial permeability of Red Wildmoor sandstone (from Holt 1990)

this is grain crushing. Beyond the critical pressure for grain crushing a further decrease of permeability takes place (David et al. 1994). Holt (1990) showed for the Red Wildmoor sandstone (Triassic, 25% porosity) that the higher the initial permeability, the lower the reduction during the hydrostatic stress increase from 3.45–34.5 MPa (Fig. 3). This suggests that the lower the initial permeability, the more stress-sensitive is the sandstone.

Stress path experiments
Rhett and Teufel (1992a, 1992b) determined the effect of stress-path loading on the matrix permeability and compressibility of reservoir sandstones. Two North Sea reservoir rocks, a poorly sorted conglomerate with 13–20% porosity and a second one, a well-sorted, medium-grained carbonate-cemented sandstone with 15–24% porosity were analysed. The first rock was cemented mainly by quartz, which is also frequently found as overgrowth material on quartz grains. Dissolved feldspar grains result in secondary porosity. The emphasis of the experiments was the possibility that reservoir stress paths may neither follow a constant stress boundary condition nor a uniaxial strain boundary condition, which may have a significant influence on the permeability evolution in the reservoir.

Permeability was measured during a series of stress-path compression test. These tests were run starting at the initial reservoir conditions (effective overburden stress: 69 MPa, effective confining pressure: 11 MPa) and then the pore pressure was reduced in increments of 6.9 MPa while the total axial stress was kept constant and the confining pressure adjusted to maintain the desired stress path K.

The algorithm used for controlling the confining pressure was:

$$Pcon_i = Pcon_0 + (Ppore_i - Ppore_0) * (1 - K) \qquad (7)$$

with $Pcon_i$ confining pressure required to follow stress path K, $Pcon_0$ the confining pressure under initial condi-
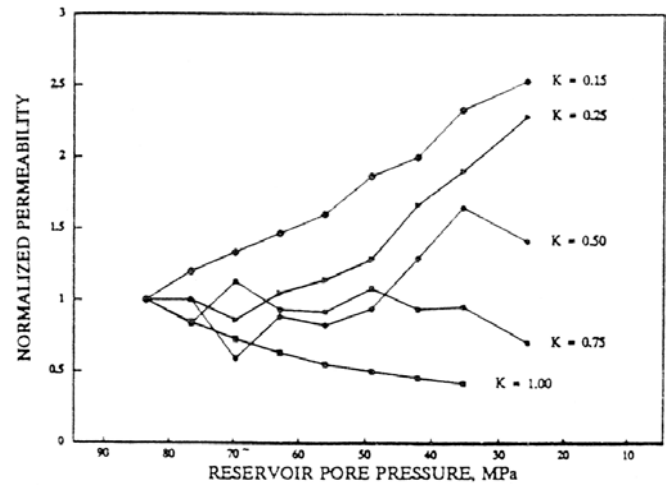

Fig. 4 Variations of normalized permeability due to loading with different stress paths (here denoted K; from Rhett and Teufel 1992b)

tions, $Ppore_i$ current pore pressure, $Ppore_0$ pore pressure under initial conditions and K the desired stress path.

Permeability measurements showed a continuous decrease in permeability for hydrostatic conditions ($K=1$). With diminishing K the amount of permeability reduction decreased until at a K between 0.75–0.5, the permeability started to increase (Fig. 4). The mechanism for this increase was not explained by the authors. However, it was stated that nearly no dilation occurred during the tests and increasing shear stress was a possible explanation for the permeability increase.

Similar experiments were reported by Ruisten et al. (1999), with the main focus on the compressibility of reservoir sandstones undergoing different stress-path experiments. Stress-path experiments were conducted on Jurassic sandstones from the Oseberg oilfield in the Norwegian North Sea. The rocks examined were the weakly cemented Etive sandstone (porosity about 25%) and the more cemented Tarbert sandstone with 21% porosity. The experimental procedure was as follows: the samples were loaded to the initial reservoir conditions of about 20 MPa effective vertical stress, 10 MPa effective confining pressure and 30 MPa pore pressure. While holding the vertical stress constant, the pore pressure was reduced and the confining pressure was controlled in such a way that the loading followed the desired stress path. The stress paths examined were $K=0$ (the lowest stress path, confining pressure stayed constant at the initial reservoir conditions, 'constant stress boundary'), $K=0.5$, $K=1$ (hydrostatic compression, the highest stress path) and uniaxial strain conditions.

Results showed a pronounced difference in the compaction and permeability behaviour between the two sandstones. The weakly cemented Etive sandstone showed increasing compressibility with decreasing stress path. The permeability of this sandstone decreased for all stress paths, with a very pronounced step-like decrease for the constant stress boundary condition ($K=0$). Results

Fig. 5 Plots of normalized permeability vs. pore pressure drawdown for laboratory stress path experiments (stress path her denoted R), k_h horizontal permeability, which is vertical to σ_1, k_v: vertical permeability (parallel to σ_1) (from Khan and Teufel 2000)
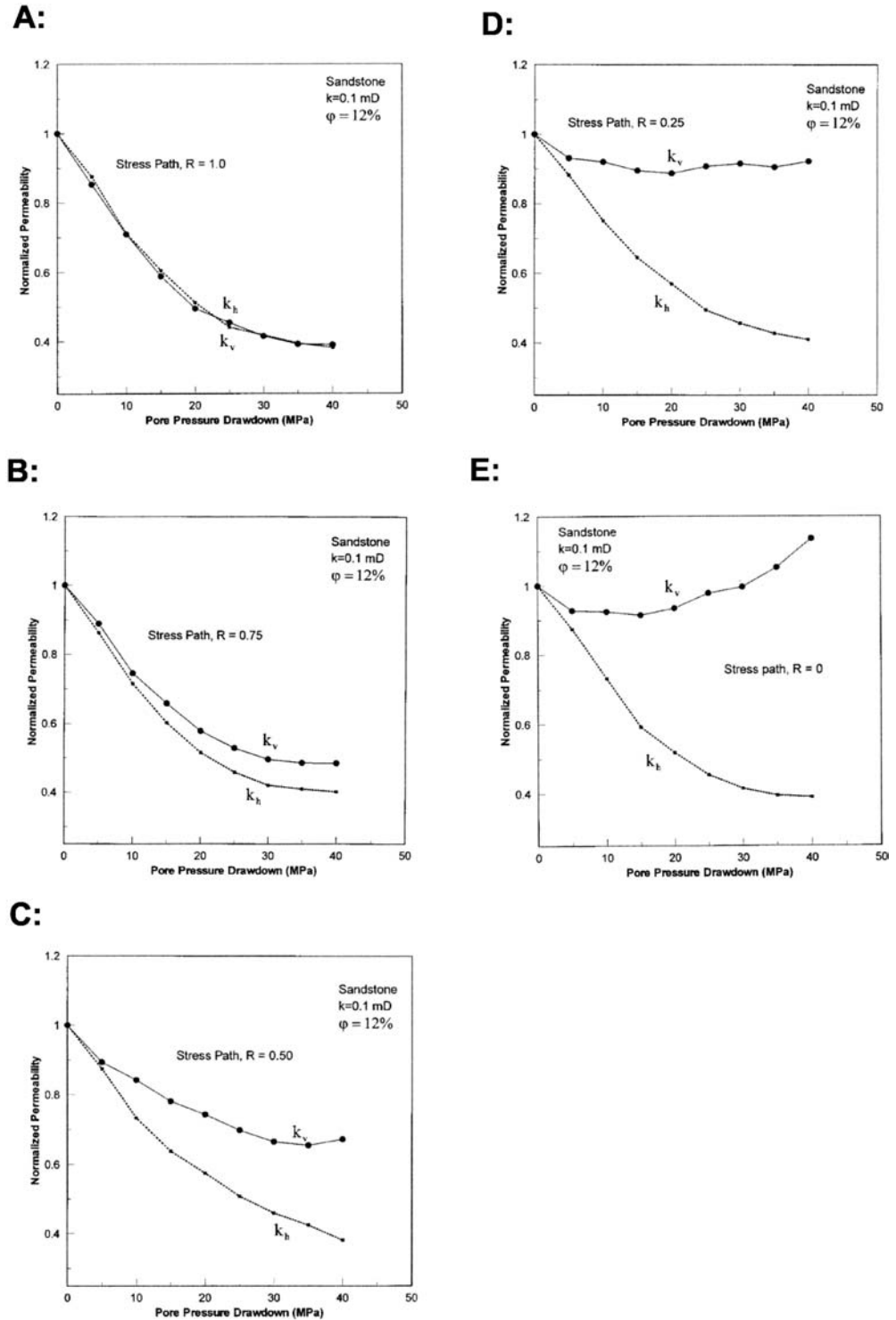
also showed a sudden permeability drop when the shear stress exceeded the yield strength and pore collapse occurred.

According to Ruisten et al. (1999), the stronger Tarbert sandstone showed decreasing compressibility with a decreasing stress path. The permeability reduction was generally smaller than for Etive sandstone, with the highest reduction taking place during the highest stress path, which is the opposite permeability development to the weaker sandstone. It was shown that for a stress path $K=0$, the permeability maintains its initial value throughout the whole test, which is believed to reflect the growth of microfractures parallel to the loading direction. At this stress path brittle failure was observed.

Khan and Teufel (2000) investigated the development of a permeability anisotropy caused by increasing differential stress. Experiments on a low-permeability sandstone with constant stress paths between $K=1$ and $K=0$
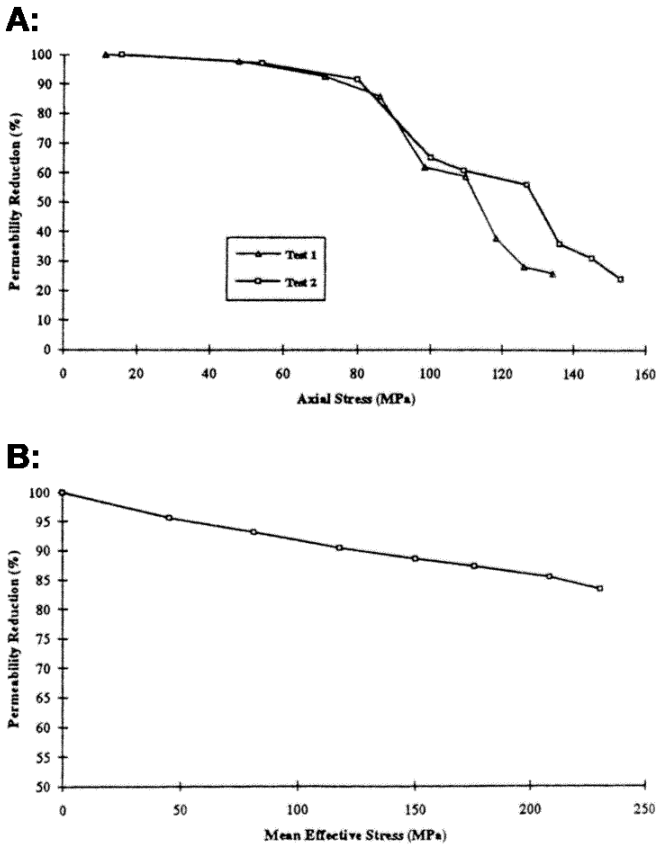
A:

B:

Fig. 6 Permeability reductions during uniaxial strain tests: **A** Indiana limestone, **B** Berea sandstone (from Azeemuddin et al. 1995)

showed that the permeability decreased with an increased effective stress, but the magnitude of permeability reduction was less in the direction parallel to the maximum stress (Fig. 5). It was further stated that the stress sensitivity of the matrix permeability of porous rocks decreased with increased permeability. In high-porosity sandstones, the stress path had little effect on the permeability, as long as the deviatoric stress did not exceed the yield strength of the rock. Beyond the yield strength, they found that a strong reduction in permeability occurred.

Uniaxial strain tests
A special case of the stress-path test is the uniaxial compression test where, starting at a hydrostatic stress state, the pore pressure is constantly reduced at constant axial stress and at constant radial strain, which is controlled by the confining pressure. Azeemuddin et al. (1995) conducted experiments of this type on Indiana limestone and Berea sandstone. Results for Indiana limestone showed pore collapse at an axial stress of about 80 MPa, whereas Berea sandstone underwent pure compaction up to an effective mean stress of 200 MPa. Consequently, the permeability of Berea sandstone showed a continuous decrease during uniaxial compression, whereas the permeability reduction of Indiana limestone suddenly accelerated when the yield strength was reached (Fig. 6).
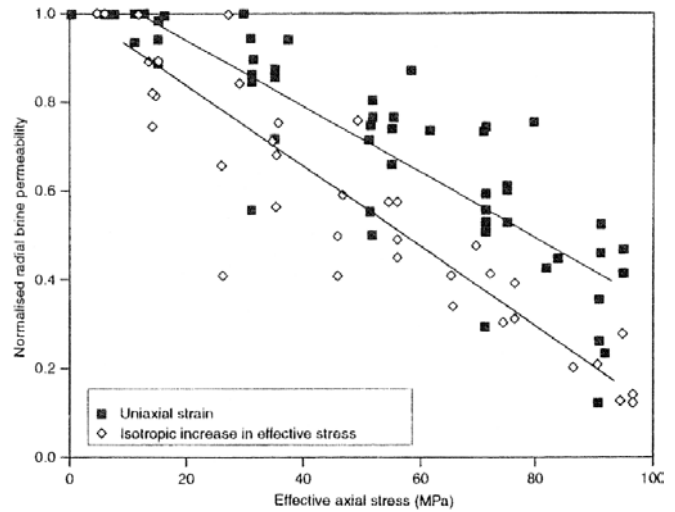

Fig. 7 Normalized radial permeability as a function of effective axial stress (from Schutjens and de Ruig 1997)

Another set of data is described by Schutjens and de Ruig (1997) from hydrostatic and uniaxial compression tests on reservoir sandstones. A special feature of the experiments was the measurement of permeability in the radial direction. Results showed an increase in axial compressibility under uniaxial strain conditions at about 60 MPa, which was linked to intergranular and transgranular fracturing found in a microscopical analysis of the samples. Radial permeability decreased under both stress paths, with a stronger decrease under hydrostatic compression (Fig. 7).

These results are similar to those of Morita et al. (1992), who also did uniaxial compression tests on Berea sandstone. It was reported that, under uniaxial compaction, the permeability evolution is qualitatively similar to the hydrostatic permeability evolution. However, compared with hydrostatic compression, it was shown that, under uniaxial strain conditions, total permeability loss is lower.

*Conclusions for the stress-path experiments
(including hydrostatic compression)*
Several authors (Morita et al. 1992; Azeemuddin et al. 1995; Schutjens and de Ruig 1997; Ruisten et al. 1999) have reported that permeability continuously decreases for all stress paths and for all sandstones investigated. Permeability reduction is the highest for a stress path of $K=1$, i.e. hydrostatic compression, and lower stress paths tend to cause less permeability reduction (Morita et al. 1992; Ruisten et al. 1999). At stress paths of $K\neq1$ increasing differential stress may reach the yield strength of the rock, which always causes a pronounced drop in permeability (Azeemuddin et al. 1995; Ruisten et al. 1999).

Rhett and Teufel (1992a, 1992b) and Khan and Teufel (2000) have shown that with decreasing stress path K the amount of permeability reduction decreases and that, be-

Fig. 8 A Stress-induced permeability reduction for Castlegate sandstone, **B** anisotropic permeability hysteresis of Castlegate sandstone (from Bruno et al. 1991)
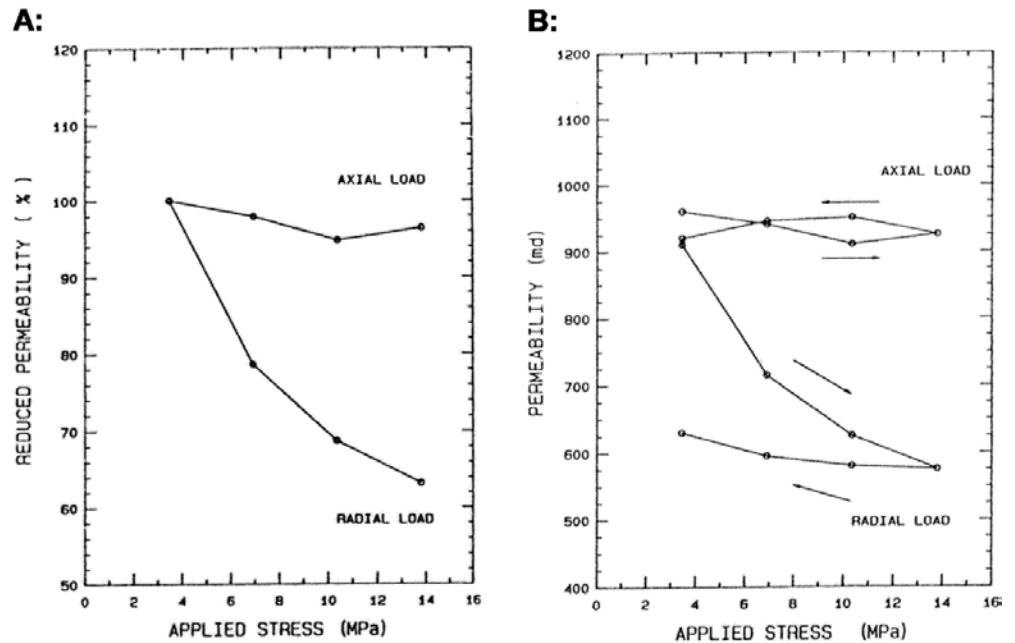
low a specific value of K, permeability increases. Khan and Teufel (2000) also show that the permeability perpendicular to the maximum stress is much less stress sensitive than the permeability parallel to it.

Group B: Experiments with Triaxial Load Conditions
Triaxial compression tests
Triaxial compression tests are the most commonly performed, non-hydrostatic tests in a rock mechanical laboratory and, thus, a large number of publications were found for this experiment type. Due to the large number of publications it was useful to structure the section according to rock types.

High-porosity sandstones (15–35% porosity)
A large number of experiments are reported for sandstones (and a few other rock types) in this porosity range. Bruno et al. (1991) investigated the permeability hysteresis of different types of sandstones (Kern River, Salt Wash and Castlegate sandstone; porosity range 15–20%) when subjected to triaxial stress. The stress difference reached during experiments was very low, only 15 MPa maximum stress at a minimum (confining) stress of 3 MPa. At the beginning of the experiments, samples were subjected to an initial hydrostatic pressure of 3 MPa. The following differential loading took place in two cycles: In the first cycle, axial stress was increased in steps of 3 MPa to a maximum of 15 MPa and in the same manner decreased. In the second cycle, the confining pressure was increased to 15 MPa and again decreased. Results showed a pronounced reduction of permeability when the rocks were loaded perpendicular to the flow direction, whereas the reduction of permeability under a load parallel to the fluid flow was much less pro-

nounced (Fig. 8A). After unloading, the samples showed a pronounced permeability hysteresis when loaded laterally, whereas the axial loading caused much less remaining permeability loss (Fig. 8B). In general it was found that the stress sensitivity of the permeability increased with decreased cementation of the rocks.

Morita et al. (1992) conducted several types of experiments on Berea sandstone (20–25% porosity). During each experiment, radial and axial permeability, pore volume change, seismic wave velocities and electrical resistivity were measured. The results of triaxial compression tests showed, first, a decrease in axial permeability followed by an increase of axial permeability well before failure of the specimen was reached.

Holt (1990) is one of the few authors who has measured permeability continuously while deforming a rock sample. A set flow-rate of 2 cm³ min⁻¹ was used, which resulted in a pressure difference of about 0.5 MPa and the samples were deformed with an axial strain rate of 5×10^{-4} s⁻¹. The rock material investigated was the Red Wildmoor sandstone, a Triassic sandstone outcropping in the UK. Its petrophysical and mechanical properties correspond to North Sea reservoir rocks, with a uniaxial compressive strength (UCS) of about 5–15 MPa and a porosity of about 25%. Using standard measurements, Holt (1990) found a strong permeability anisotropy with Klinkenberg-corrected gas permeability being 1–1.5 Darcy along bedding and 0.1–0.5 Darcy perpendicular to bedding. The results of the triaxial tests were (Fig. 9): Permeability decreased under non-hydrostatic stress and, as long as the stress was smaller than the yield stress, the amount of decrease was similar to the permeability reduction due to hydrostatic loading. Yield occurred mostly around 1% axial strain and, after the onset of yielding, the rate of permeability reduction increased sharply and permeability decrease continued un-

til failure. The amount of permeability reduction varied between 10–95%, with the higher reductions at higher confinements. Even though at low confining pressures (~5 MPa), brittle failure occurred, Holt could not find any sign of dilatant behaviour, either from strain or from permeability measurements. At higher confining pres-

sures (>30 MPa), the failure mechanism became more and more ductile.

Another set of experiments was described by Azeemuddin et al. (1995); triaxial tests were conducted on Indiana limestone and Berea sandstone, both with 18% porosity. Results showed that the permeability of Indiana limestone decreased continuously in triaxial compression, which corresponds to ductile (cataclastic) stress–strain curves (Fig. 10A). Berea sandstone showed brittle behaviour in triaxial compression with permeability decrease during compaction and permeability increase after the onset of dilatancy (Fig. 10B).

Wong et al. (1997) and Zhu and Wong (1997) examined the transition from brittle faulting to cataclastic flow in high-porosity sandstones and permeability development during this process. Triaxial compression experiments were conducted on several sandstones with confining pressures between 13–550 MPa, a fixed pore pressure of 10 MPa and an axial strain rate of 5×10^{-5} s^{-1}. The investigated sandstones were (among others) Darley Dale (14.5% porosity), Berea (21% porosity) and Boise (35% porosity). At low confining pressures, the samples showed brittle failure, which is associated with dilatant deformation. At higher confining pressures, the samples showed constant compaction, which is representative of the cataclastic flow regime. The permeability evolution shows continuous reduction for both deformational regimes for the high-porosity sandstones. Zhu and Wong
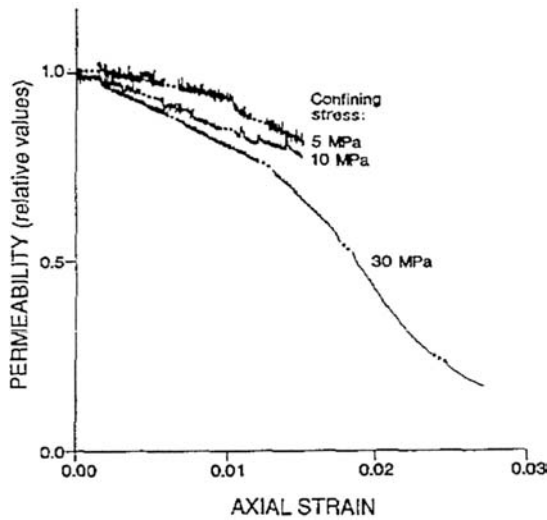

Fig. 9 Relative permeability change during triaxial compression tests with the Red Wildmoor sandstone at three confining pressures and with flow parallel to bedding (from Holt 1990)

Fig. 10A, B Permeability reductions during triaxial tests. **A** Indiana limestone (the legend shows the different effective stresses of the experiments), **B** Berea sandstone (from Azeemuddin et al. 1995)
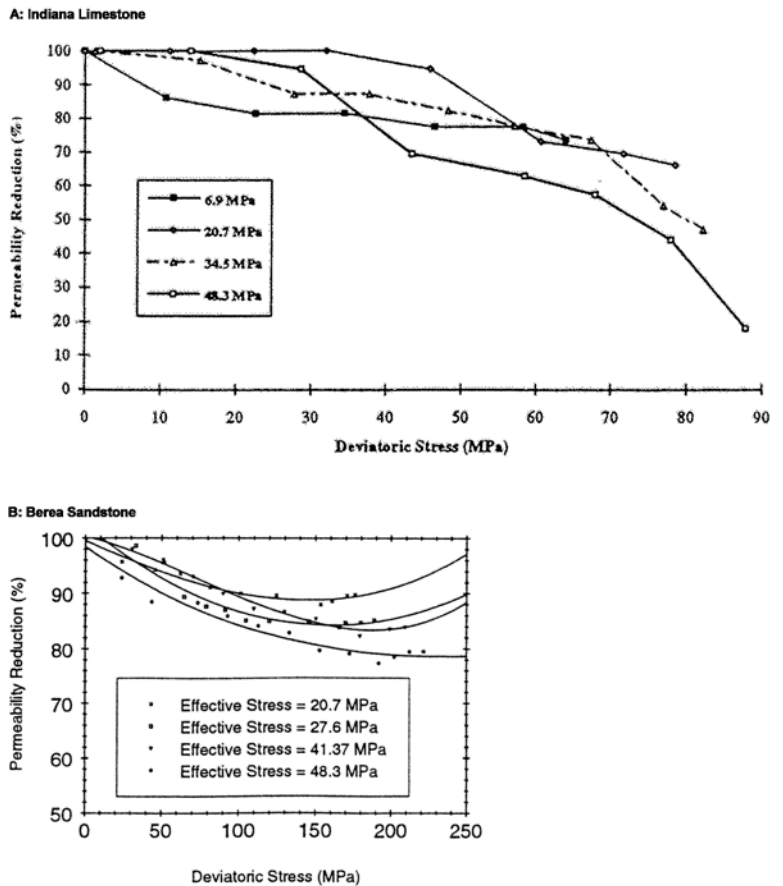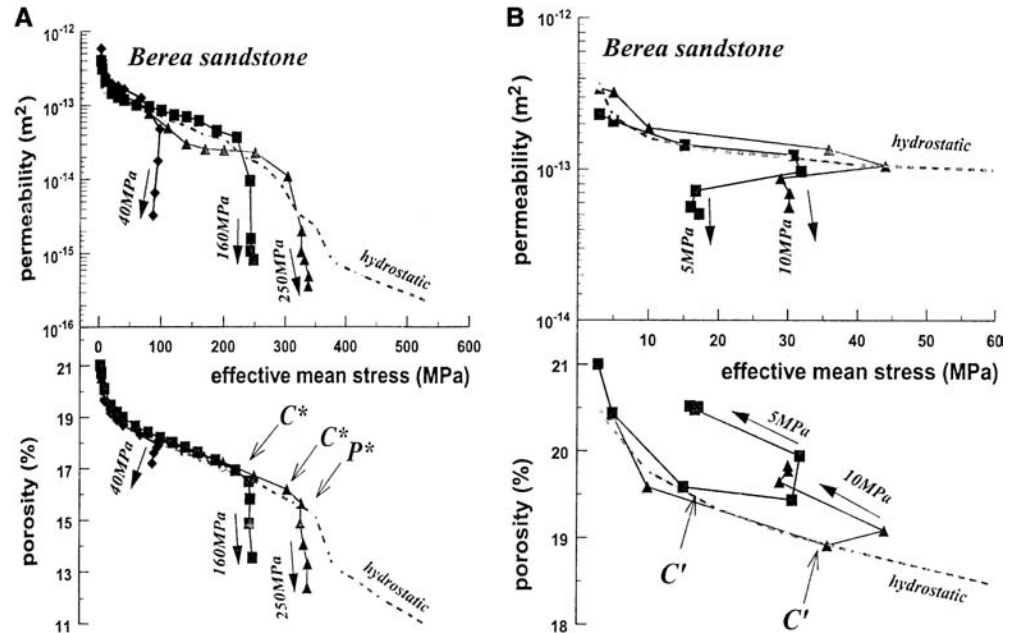
Fig. 11 Permeability and porosity vs. effective mean stress, triaxial tests on Berea sandstone: **A** cataclastic flow regime, **B** brittle regime (from Zhu and Wong 1997)

(1997) showed that the permeability vs effective mean stress curves of all examined sandstones follow the trend of hydrostatic permeability evolution up to a specific stress level. In the cataclastic field, a sudden drop in permeability occurred at this level; the stress level at which the permeability drop occurred depended on the confining pressure: the higher the σ_3, the higher the critical stress level (Fig. 11).

Zhu and Wong (1997) also report that, in the brittle field, Darley Dale sandstone, the one with the lowest porosity, showed decreasing permeability until the onset of dilatancy and a slight increase in permeability afterwards. From this, Wong and his co-workers (Wong et al. 1997; Zhu and Wong, 1997) concluded that the permeability evolution of sandstone in the brittle field is different for low-porosity than for high-porosity sandstones. Below 15% porosity, permeability increased after the onset of dilatancy whereas, above 15% porosity, the permeability constantly decreases, even when dilatancy (i.e. porosity increase) occurs.

Low-porosity sandstones (porosity <10%)
Personal research was focused on a fine-grained and well-consolidated low-porosity (6.5–9%) sandstone of Lower Permian age, with permeability on the order of 10^{-15} m^2 (milliDarcy). Blocks of Flechtinger Bausandstein sandstone were sampled in a quarry near Magdeburg in Germany, situated about 100 km south-west of Berlin.

The specimens used for the triaxial tests were drilled from rock blocks, which had been taken from the quarry face using a chisel and hammer. The specimens had a diameter of 50 mm and a length of 100 mm. The end-planes were ground smooth and vertical to the cylinder axis. The specimens were saturated with de-ionised water under vacuum for a minimum of 48 h. Porosity and unit weight were determined by weighing the sample dry, saturated and under buoyancy.

Triaxial testing equipment and procedures used in personal research. For isolation from the confining pressure medium (a high-temperature silicone oil), a shrinkable Teflon sleeve was put around the specimen and the extensometers for strain measurements were clipped on the jacket. All experiments were done under either 10 or 20 MPa confining pressure, which means that these experiments only covered the brittle deformation field.

The pore pressure was applied using four independently controllable syringe pumps, which were controlled by a computerized system. The fluid pressures were controlled in such a way that fluid was pumped through the specimen from bottom to top with a pressure difference of 1 MPa over the sample length and a total pore pressure (at the fluid inlet) between 80–90% of the confining pressure. Applying a constant differential pressure and measuring flow rate resembles the natural conditions, where fluid flow is assumed to be controlled by pressure differences.

When total equilibrium of the pore pressure, flow rates and hydrostatic pressure was reached, the specimen was loaded axially, that is parallel to the flow direction, in lateral strain control. Figure 12 shows a schematic sketch and pictures of the experimental equipment of the rock mechanics laboratory at GeoForschungsZentrum Potsdam, where the experiments described in this section were conducted.

The experiments were conducted in a triaxial testing system consisting of a stiff loading frame and a triaxial cell with a maximum confining pressure of 140 MPa. The triaxial cell was equipped with in-vessel sensors, which allow very precise measurement of axial force and
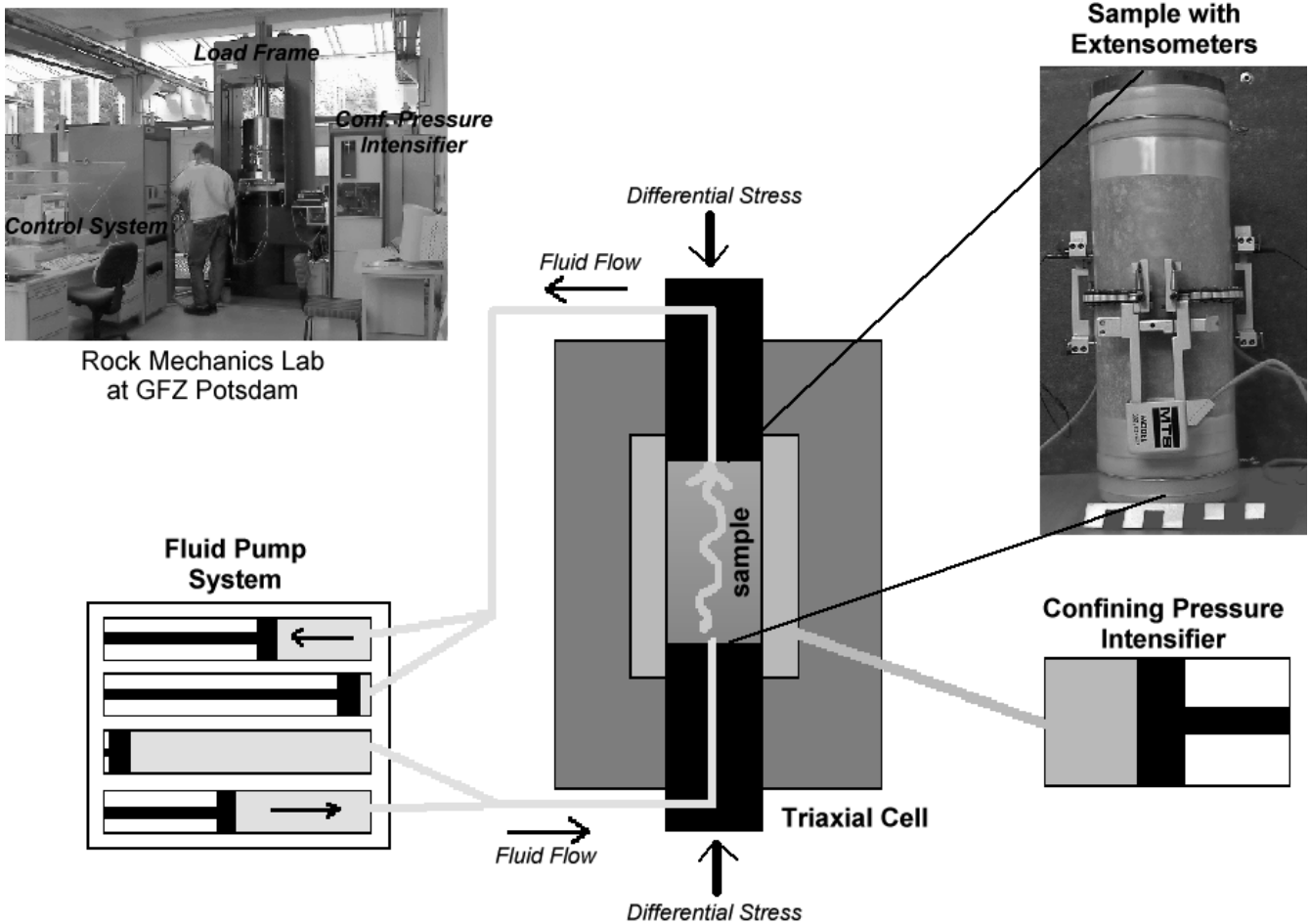
Fig. 12 Schematic sketch and pictures of the equipment of the rock mechanics laboratory at GeoForschungsZentrum Potsdam

sample deformation. Axial strain was detected with two extensometers located 180° from each other on the sides of the specimen. They measure axial strain over a length of 50 mm in mid-height of the specimen. Lateral strain was calculated from measurements of a circumferential extensometer. The readings of both axial and lateral strain were used as a feedback signal for force control. Volumetric strain was calculated from the strain measurements using the equation:

$$\varepsilon_{vol} = \varepsilon_{ax} + 2 \cdot \varepsilon_{lat} \qquad (8)$$

with ε_{vol} volumetric strain, ε_{ax} axial strain and ε_{lat} lateral strain.

As is usual in rock mechanics, axial strain (shortening of specimen length) is positive, lateral strain (thickening of the specimen) is negative and compression is positive. Based on Eq. (8), increasing volumetric strain indicates compaction, decreasing volumetric strain indicates dilatancy.

Usually, the experiments were done in lateral strain control with a strain rate between 10^{-6}–10^{-7} s^{-1}. Lateral strain control is preferred because in this control mode dilatant sample deformation can be controlled more pre-cisely than in axial strain control. In addition, lateral strain was measured around the whole circumference of the sample and, thus, deformation was detected wherever the shear surface developed. In contrast, the axial extensometers measured between two pins at 50 mm distance and were located at the side of the specimen cylinder. Depending on the location of the shear fracture, deformation in the post-failure region may not be detected by one or both axial extensometers.

The experimental set-up facilitates permeability measurements using the steady-state method while continuously deforming the sample at very low strain rates (10^{-6} s^{-1}). To investigate the difference between permeability measurements during actuator stops and during continuous deformation, two experiments were conducted, where permeability was measured continuously and the actuator was stopped at different levels throughout the test. One test was done on limestone by just stopping actuator movement for a specific time and the other test was done on sandstone by simultaneously restricting lateral strain by adjusting the confining pressure ('zero-strain' condition). However, from the plots, it can be see that, at higher stress levels (close to sample failure), no stable boundary conditions could be established within the sample (Figs. 13 and 14).

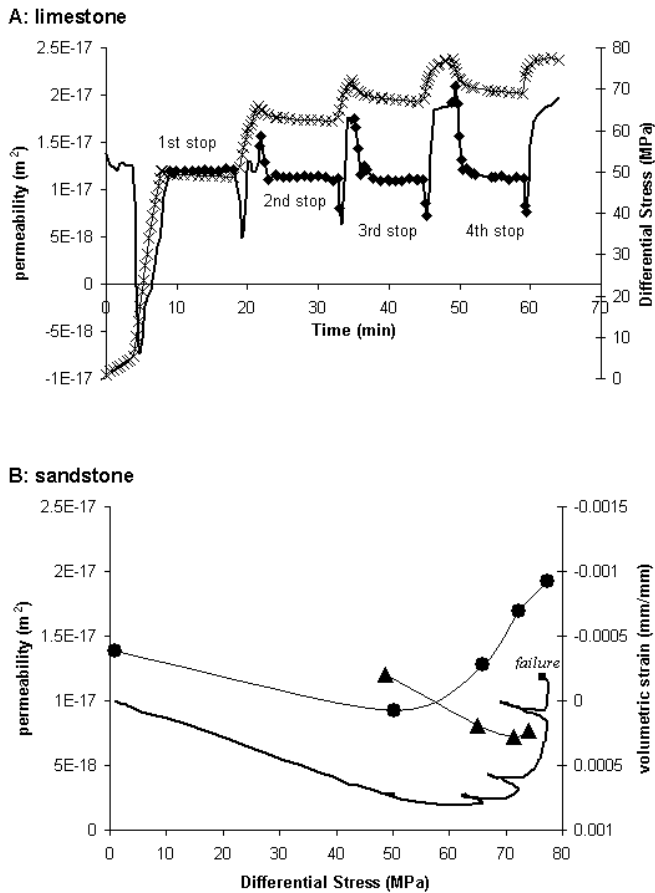Several observations could be made throughout these tests:

A: limestone

B: sandstone

Fig. 13 A Time development of axial stress and permeability for Rüdersdorfer limestone, triaxial test with stopped actuator movement at specified stress levels, permeability values measured during the stops are marked by *diamonds*. **B** Permeability and volumetric strain vs. differential stress, permeability values shown at beginning of each stop (*circles*) and at end of each stop (*triangles*)

1. Rüdersdorfer limestone
   – Each change in the loading regime (starting axial loading, stopping actuator movement, continuing actuator movement) leads to a strong, transient change in permeability (spikes in permeability vs time curve). This transient change was probably linked to pore-pressure changes generated by the switch in the loading conditions (stop of loading and continuation of loading).
   – During all stops, stable flow rates could be achieved.
   – Before the onset of dilatancy, the permeability is constant when the actuator movement is stopped (first stop).
   – After the onset of dilatancy (which happened between the first and second stop) the limestone shows pronounced stress relaxation when the actuator was stopped, which led to very high permeability drops (Fig. 13A).
   – The permeability values measured during loading of the sample started to increase with the onset of dilatancy (Fig. 13B, circles).
   – The permeability measured during the stops started to increase just as peak strength was reached (Fig. 13B, triangles).

2. Flechtinger Bausandstein sandstone with 'zero-strain' condition during stops.
   – Stress relaxation was nearly totally suppressed by the confining pressure adjustment.
   – Consequently the permeability did not change during stops (before onset of dilatancy) (Fig. 14, stops 1 and 2).
   – At the onset of dilatancy the confining pressure adjustment necessary for keeping "zero-strain" conditions lead to a pronounced, non-transient drop in permeability (Fig. 14, 3rd stop).
   – After peak strength, the actuator stop caused a transient permeability decrease (Fig. 14, 4th stop).

Fig. 14 Triaxial test on Flechtinger Bausandtein sandstone, experiment with 'frozen' deformation during actuator stops
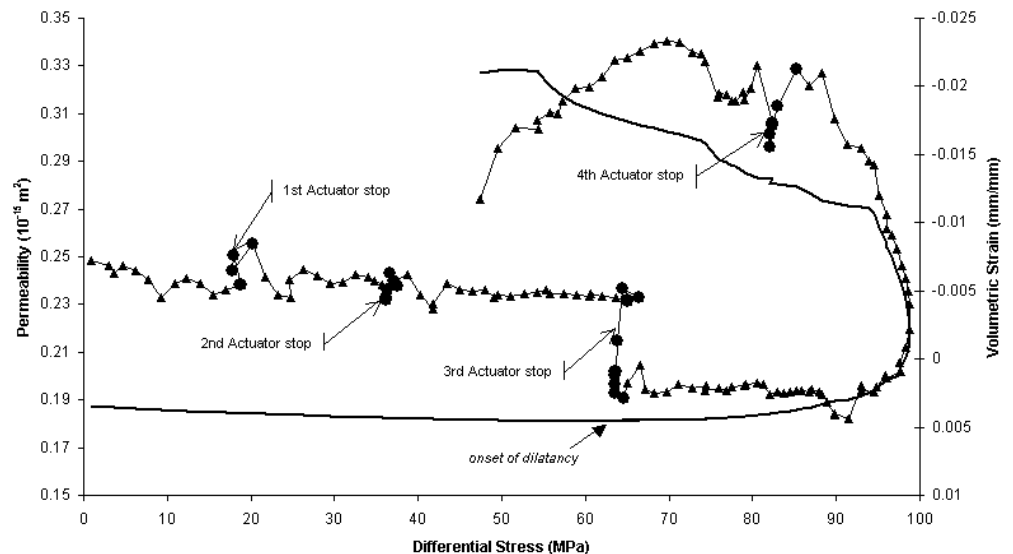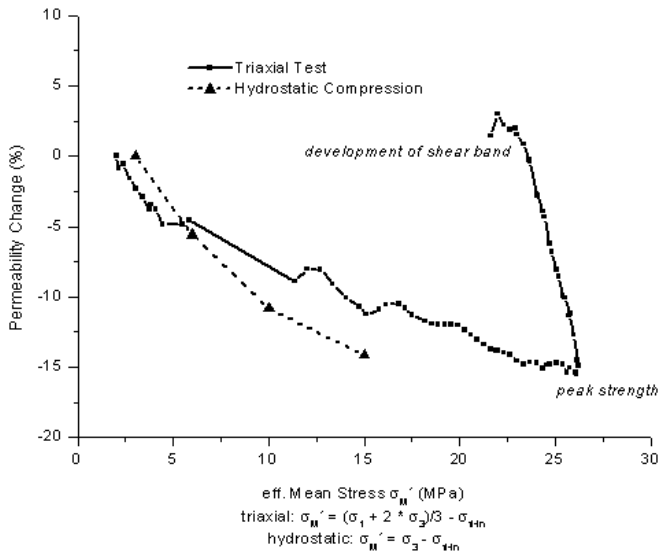
Fig. 15 Permeability vs. stress plot for Flechtinger Bausandstein sandstone, shown are data from one triaxial test and one hydrostatic compression test

Following these experiences, it was decided to conduct the triaxial experiments with continuous permeability measurement during continuous loading of the sample. In order to avoid a strong transient disturbance of the flow rates at the beginning of the axial loading, the triaxial loading was started as smoothly as possible by slowly increasing loading up to the final value of 3×10^{-6} s^{-1}.

Results of personal research. For two samples the permeability reduction under hydrostatic compression was measured and compared with the influence of triaxial compression on permeability. Heiland and Raab (2001) showed that the permeability change during the compactional phase of a triaxial test is similar to the permeability reduction due to increasing effective stress under hydrostatic conditions (Fig. 15). As this was found to be valid by many authors (e.g. Zhu and Wong 1997), it can be taken as proof that permeability can be determined using steady-state fluid flow while continuously deforming the sample in a triaxial cell.

In general, the permeability evolution during the presented triaxial tests is similar to the descriptions of most authors for brittle deformation: a permeability reduction during the early stages of differential loading and a later increase in permeability (see Fig. 16). However, from the permeability vs. differential stress plots, the onset of permeability increase cannot clearly be linked to a specific event. When plotting permeability vs. volumetric strain (Fig. 17), the link between permeability evolution and deformation becomes clearer. At the onset of dilatancy, i.e. the point with the highest volumetric strain value, the permeability evolution starts to move from a decrease to an increase. The only exception is experiment FB 3.6, where the transition from decreasing permeability to increasing permeability takes place slowly over a wider
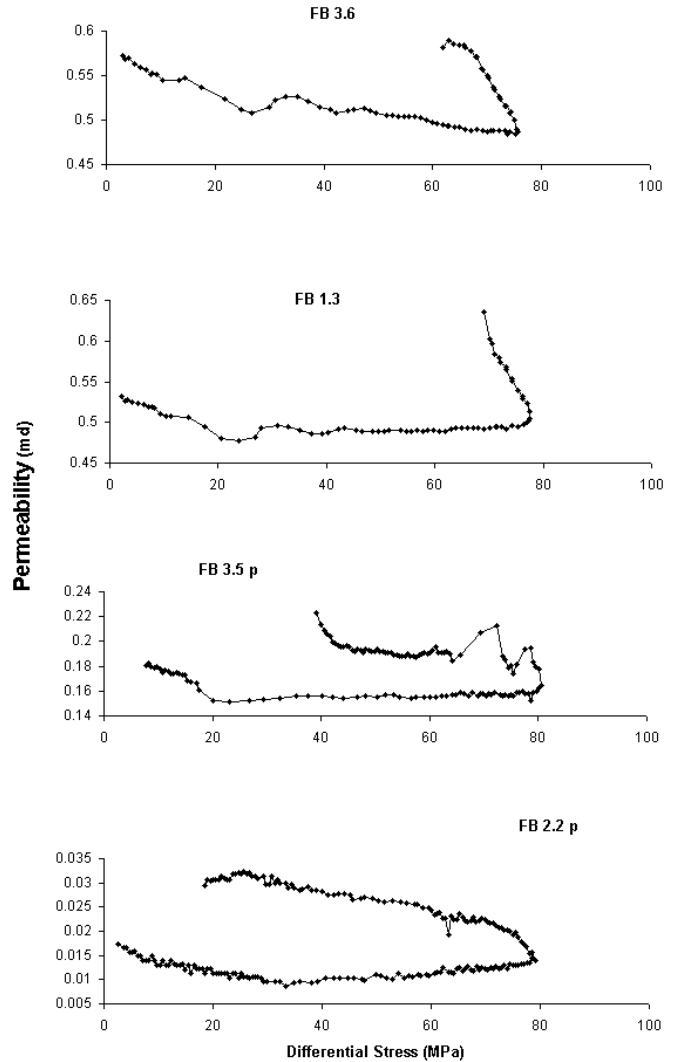

Fig. 16 Plots of permeability vs. differential stress for four triaxial tests on Flechtinger Bausandstein sandstone

range of deformation (Fig. 17). Another interesting feature can be seen in this plot: all specimens show a linear dependence between permeability and volumetric strain in the dilatant regime, with a trend similar for most of the experiments (Fig. 17).

Low-porosity sandstones in the literature. Keaney et al. (1998) reported experiments on Tennessee sandstone, a very low-porosity (4.5–7.5%), quartz-rich sandstone, with a permeability in the range of microDarcys (10^{-18} m^2) at 20 MPa-effective confining pressure. Using a transient pulse permeability measurement, and a triaxial deformation apparatus, the permeability and specific storage characteristics of this rock, when undergoing triaxial deformation, were determined. The rocks were deformed well beyond failure and into the post-failure region in order to determine the influence of shear bands on the permeability.

In addition to the triaxial tests, Keaney et al. (1998) conducted permeability measurements under hydrostatic
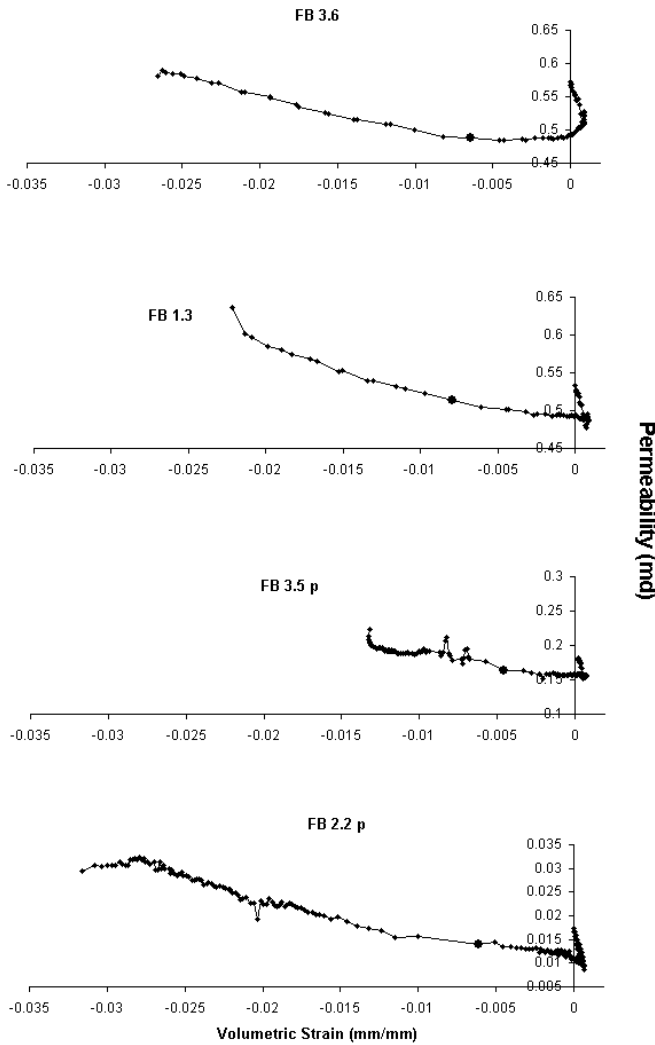
Fig. 17 Permeability vs. volumetric strain plots for the same experiments as in Fig. 16

conditions. It was reported that increasing hydrostatic pressure results in a continuous decrease in permeability and specific storage. The permeability decreased during the experiments by one order of magnitude with an increasing effective pressure of 20–80 MPa, whereas the specific storage decreased by about a factor of two over this pressure range. The rates of decrease both slow down with increasing effective pressures.

For triaxial compression tests, Keaney et al. (1998) identified five deformation phases:

1. During compaction the elastic closure of existing cracks and grain boundaries leads to a decrease in permeability and specific storage. The permeability decreased by a factor of about two during the phase.
2. When dilatancy started to dominate the deformation regime, the nucleation and growth of microcracks resulted in an increase in permeability and specific storage. Both properties increased to a value that was considerably higher than their initial values.
3. When approaching peak strength, developing microcracks were mainly aligned parallel to the maximum principle stress direction. Brittle failure of the sample was accompanied by a transient permeability peak, where permeability may increase for a short time up to a factor of 17 compared with the initial value. This behaviour was also found by the author and is shown in Fig. 18.
4. After peak strength, strain softening occurred and the deformation became highly localized; it eventually resulted in the formation of a macroscopic fracture.
5. Continuous straining resulted in frictional sliding on this fracture. At this stage, permeability reached a stable value, which was about 1.5 times higher than the initial value.

Crystalline rock

As early as 1975a, Zoback and Byerlee published a paper on the influence of dilatancy on the permeability of the Westerley granite. Samples of this rock were sub-

Fig. 18 Time development of permeability and differential stress for one triaxial test on Flechtinger Bausandstein sandstone
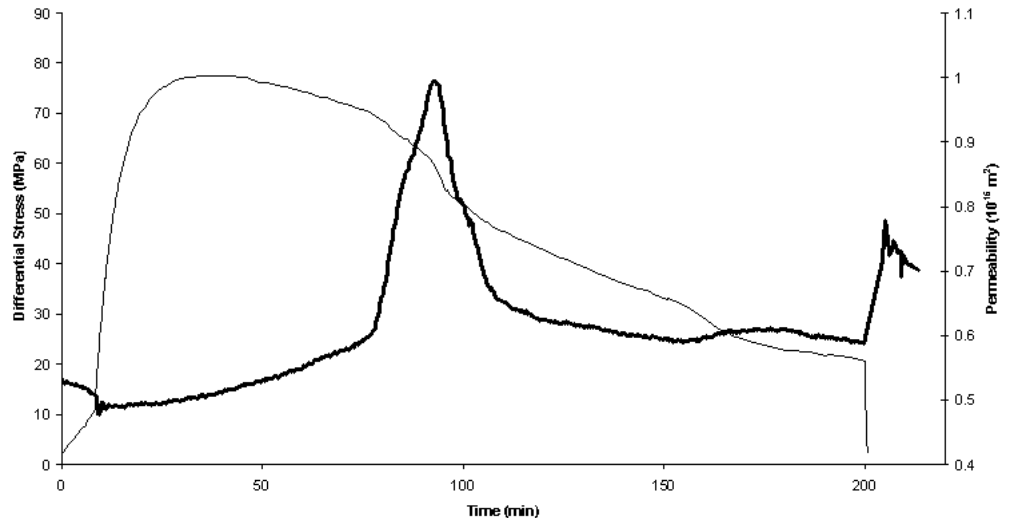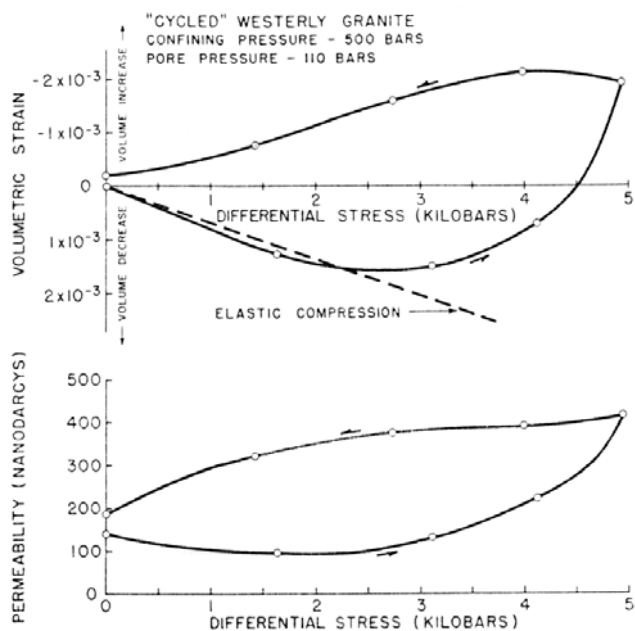
Fig. 19 Volumetric strain and permeability plotted as a function of differential stress. Triaxial tests on Westerley granite at 50 MPa confining pressure (from Zoback and Byerlee 1975a)

jected to triaxial stresses between 75–95% of their ultimate compressive strength, while measuring the permeability in the axial direction. The experiments showed a reduction of permeability in the early stages of loading, which was similar to the permeability reduction due to hydrostatic compression (Fig. 19). When the stress was increased further, the sample deformation became dilatant and permeability started to increase. At the end of the experiments, the permeability exceeded by far the initial permeability and also stayed above the initial value when the samples were unloaded.

Rocksalt

Stormont and Daemen (1992) investigated the permeability change of rocksalt samples under hydrostatic and triaxial compression. The first kind of test was intended to determine the degree of sample disturbance and how to reverse it. Triaxial tests were to determine how gas permeability changes with deformation as a function of confining pressure and deviatoric load.

Hydrostatic compression of rocksalt leads to unrecoverable volumetric strain (compaction), which is associated with permeability and porosity reduction. When the sample was unloaded this reduction did not reverse, which is referred to as 'healing' (Fig. 20A). The longer the sample stays under hydrostatic compression, the higher the degree of healing (Stormont and Daemen 1992).

Triaxial compression tests were conducted at confining pressures between 2.4–7.6 MPa and at a loading rate of 0.2 MPa min^{-1}, which resulted in an axial strain rate between 3×10^{-5}–10^{-6} s^{-1}. For permeability measurements, the axial deformation was stopped, which resulted in a re-

laxation of axial stress. Mechanically, all the experiments showed strain hardening and dilatancy when a specific level of deviatoric load was reached (Fig. 20B). The higher the confining pressure, the higher the deviatoric stress at which dilatancy started. The permeability evolution of the experiments conducted by Stormont and Daemen (1992) showed a strong increase when a certain level of strain was reached (Fig. 20C, D). Below this level, permeability could not be measured because of the tight structure of the rocks after the hydrostatic compression phase. For all confining pressures, the permeability eventually reached a stable value; the higher the confining pressure, the lower the value (Stormont and Daemen 1992).

The papers by Schulze and his co-workers (Popp et al. 1999; Hunsche and Schulze 2000) describe the correlation between increasing damage, porosity and gas-permeability of rocksalt undergoing triaxial deformation with a constant strain rate in the range of 10^{-5}–10^{-6} s^{-1}. In general, results showed decreasing permeability during compaction. The onset of dilatancy, which was paired with the onset of permeability increase, took place at about 90% of the peak strength (Fig. 21). The main conclusion was that the relation between permeability and porosity was very non-linear and varied greatly for the different types of rocksalt.

Triaxial extension tests

Holt (1990) conducted triaxial extension tests on Red Wildmoor sandstone. A triaxial extension test is done by loading the sample with a high hydrostatic pressure (normally the value of the maximum in-situ stress) and unloading it in an axial direction, while keeping the confining pressure constant. This kind of load path leads to negative axial strain (e.g. lengthening) of the sample cylinder and results in rock failure along a horizontal plane. The failure stress is a measure of the tensile strength of the rock. This failure mechanism is often assumed to resemble core disking, which occurs during unloading of cores from an originally high in-situ stress.

The experiments reported by Holt (1990; Fig. 22) started at 40 MPa hydrostatic pressure and showed a very interesting permeability evolution: During the early phase of axial unloading, the permeability stayed constant. When a certain level of differential stress and axial strain was reached, a sudden drop in permeability occurred. This happened at about 90% of the failure strength and 60% of strain to failure.

True triaxial experiments

Al-Harthy et al. (1996) conducted true triaxial experiments with gas-permeability measurements on sandstone cubes with 40-mm side lengths. The sandstone was a high-permeability outcrop rock called Doddington. The aim of the experiment was to investigate the influence of stress cycling on permeability. The general result of the experiments was that the permeability hysteresis was higher for high porosity rocks and was more pronounced
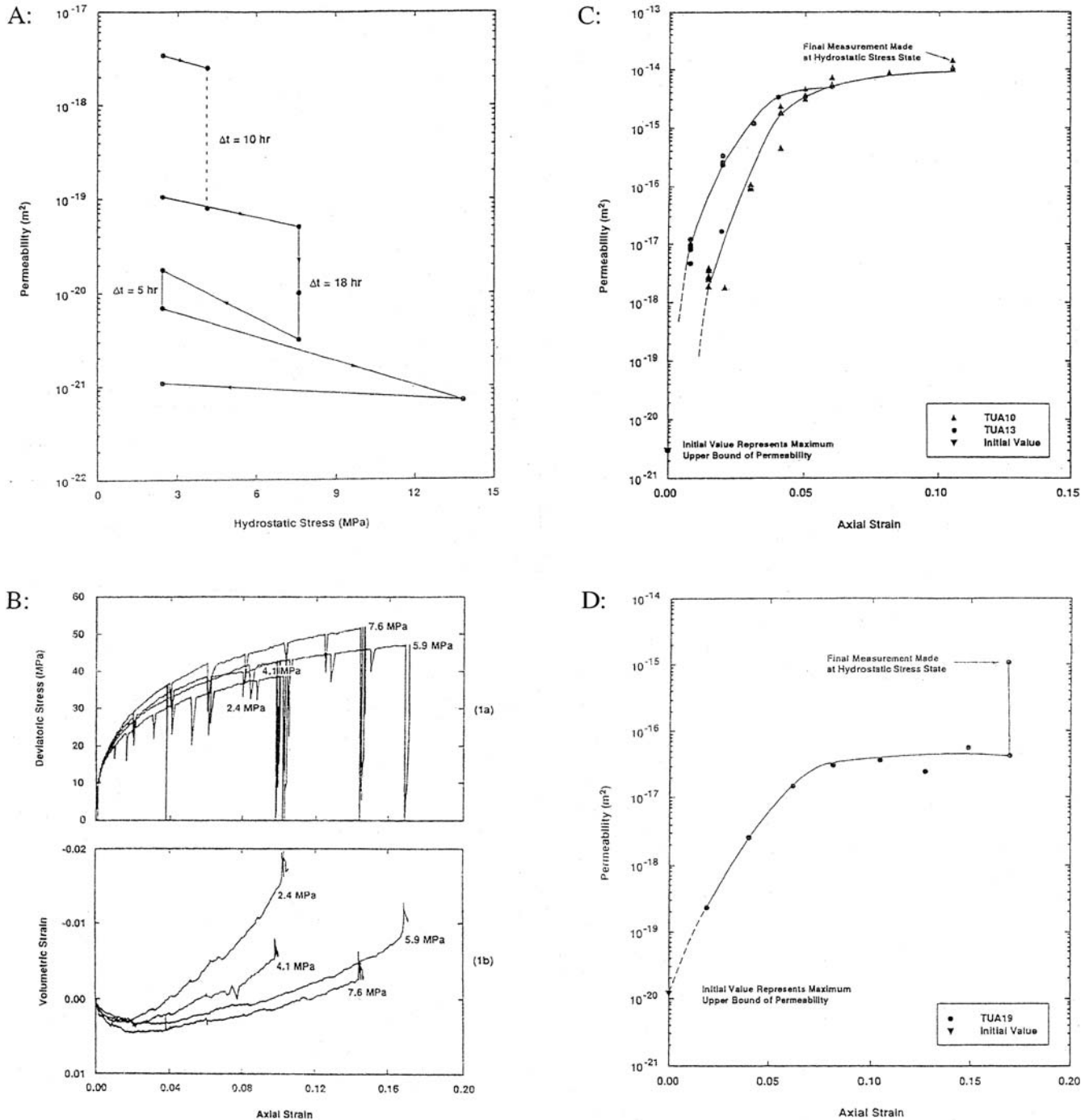
Fig. 20 A Permeability vs hydrostatic pressure plot, showing the 'healing' of a rocksalt sample due to increased hydrostatic pressure. **B** Deviatoric stress and volumetric strain vs axial strain plots for triaxial tests at different confining pressures. **C** Permeability vs axial strain plot for triaxial tests at 2.4 MPa confining pressure. **D** Confining pressure of 5.9 MPa (from Stormont and Daemen 1992)

under hydrostatic stress. Results of the experiments with loading of the samples under σ_3 constant at 3 MPa and an $\sigma_1=\sigma_2$ increase resulted in a sudden increase in permeability at about $\sigma_1=\sigma_2=100$ MPa and eventually lead to failure at about $\sigma_1=140$ MPa, whereas σ_2 was kept constant at 100 MPa (Fig. 23).

In 1998, the same authors published another paper (Al-Harthy et al. 1998) where similar results were reported for another set of sandstones. The authors stated that for true triaxial stresses, the permeability reduction due to the increase of effective stresses was higher than for hydrostatic stress conditions.

Conclusions for triaxial tests

Morita et al. (1992), Holt (1990), Azeemuddin et al. (1995), Khan and Teufel (2000), Zoback and Byerlee (1975b), Stormont and Daemen (1992), Hunsche and Schulze (2000), Popp et al. (1999), Heiland and Raab
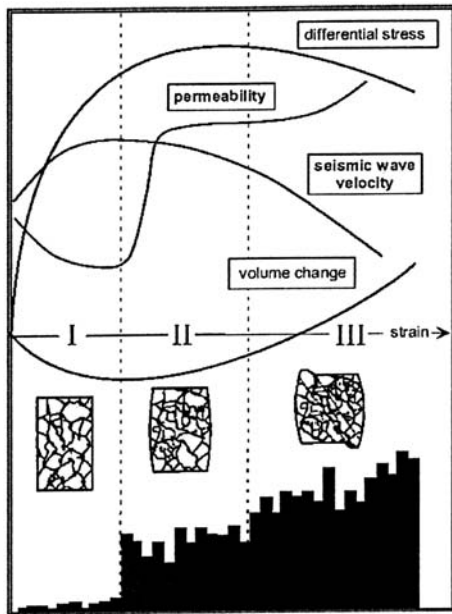
Fig. 21 Schematic plot of the mechanical and hydraulic behaviour of rocksalt during triaxial experiments (from Hunsche and Schulze 2000)
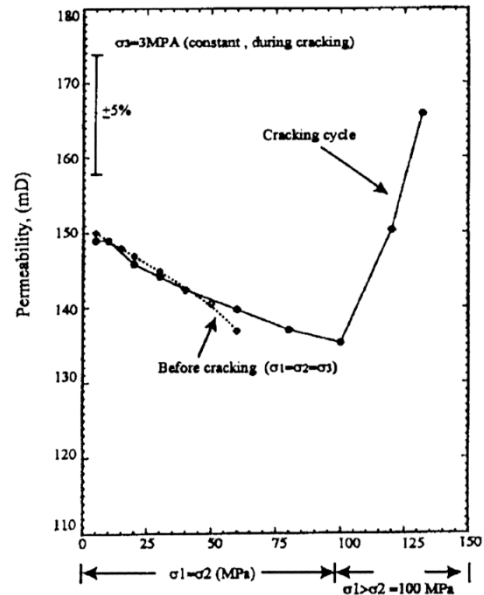

Fig. 23 Permeability vs. stress plot for a true triaxial experiment (from Al-Harty et al. 1996)
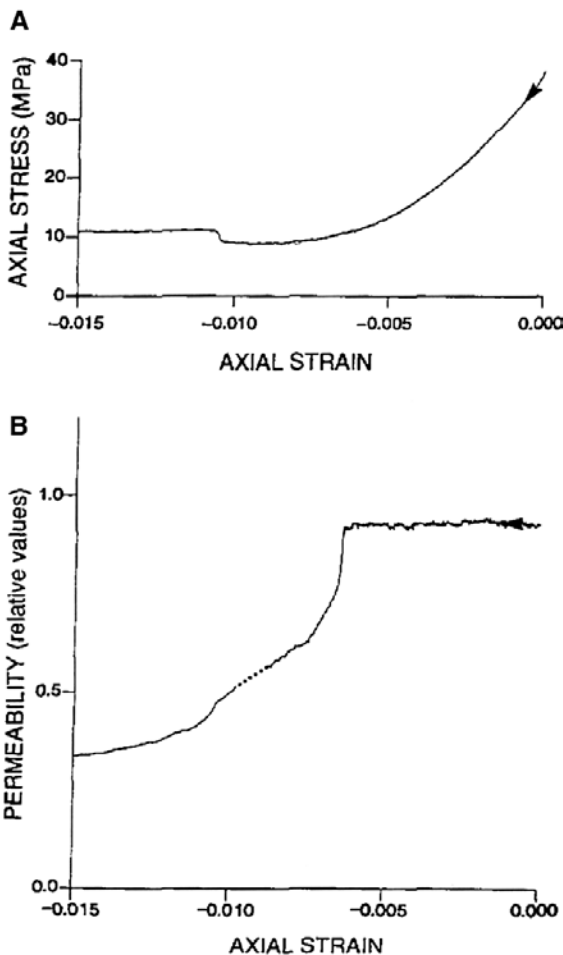

Fig. 22 Stress–strain plot for a triaxial extension test and the permeability vs. axial strain curve for the same experiment (from Holt 1990)

(2001), Wong et al. (1997), Zhu and Wong (1997) and Keaney et al. (1998) all described the influence of triaxial compression on the matrix permeability of rock and the findings of these investigations can be summarized as follows:

– In the brittle deformation field, most studies have shown decreased permeability during the early stages of the differential loading, as long as the rock deformation was compactional (Fig. 24B).
– After a specific level of differential load was reached, dilatancy occurs, which was mostly accompanied by an onset of permeability increase.
– The permeability reduction during the compactional phase was similar to the permeability reduction induced by hydrostatic compaction.
– The statements above were found valid for different rock types (sandstones of all porosity ranges, crystalline rock and rocksalt), regardless of their porosity.
– The amount of permeability increased after the onset of dilatancy varied with different rock types: for crystalline rocks the increase by far exceeded the initial permeability (Zoback and Byerlee 1975a) whereas, for sandstones, the increase did not reach the initial permeability (Morita et al. 1992; Zhu and Wong 1997; Heiland and Raab 2001).
– In the cataclastic deformation field, continuous permeability reduction takes place with an increase in the reduction rate at the onset of grain crushing (yield strength; Zhu and Wong 1997).

A contradiction in the results of several authors was found for the high-porosity sandstone Berea (18–21% porosity). Two studies showed the 'normal' permeability evolution for low confining pressures, i.e. permeability reduction
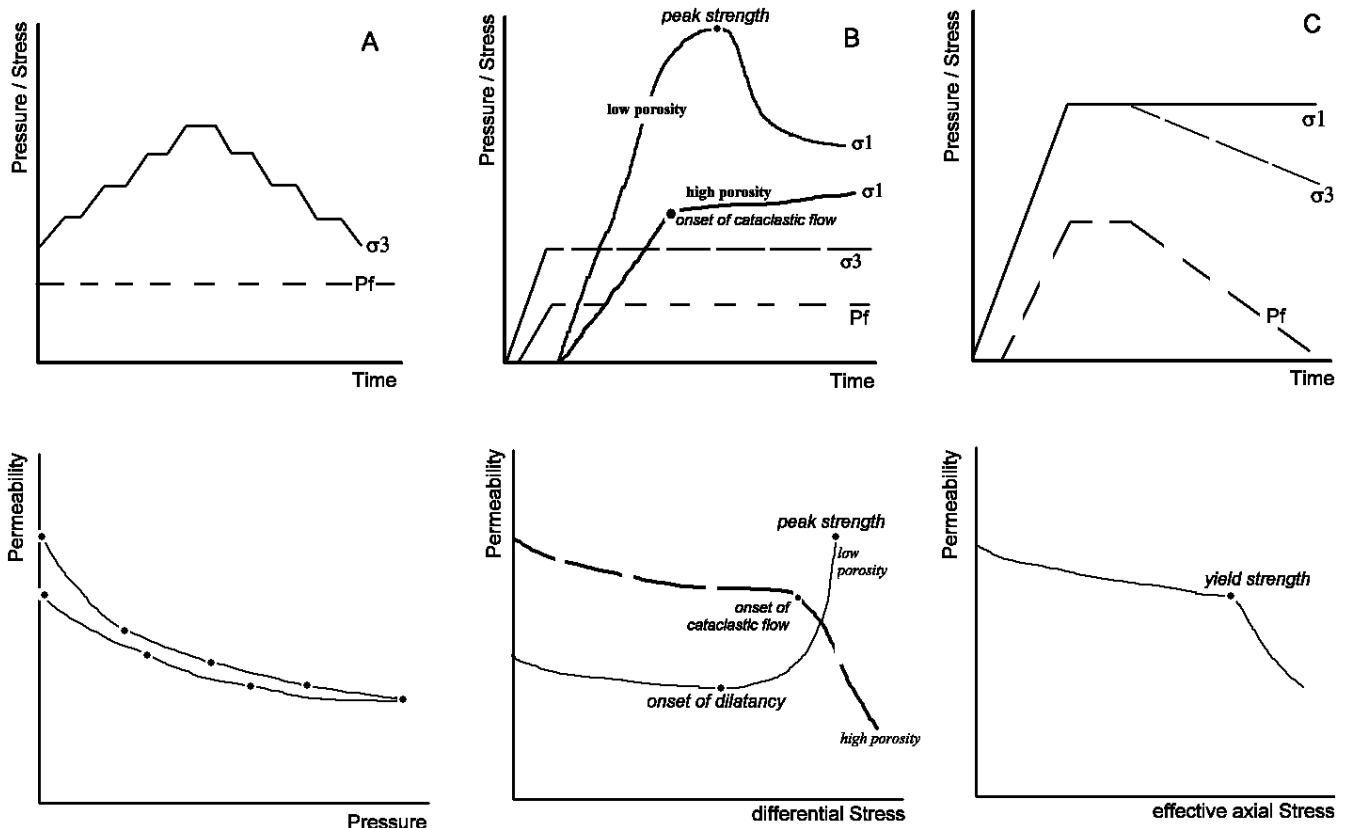
Fig. 24 Compiled results for **A** hydrostatic compression, **B** triaxial compression and **C** uniaxial strain conditions. *Upper diagrams* show the timely workflow of the experiments and the lower parts show schematic permeability vs pressure/stress plots for the main parts of the experiments

during compaction and permeability increase during dilatancy (Morita et al. 1992; Azeemuddin et al. 1995). Zhu and Wong (1997), on the other hand, showed brittle deformation associated with continuously decreasing permeability for this sandstone (and other more porous sandstones) at low confining pressures (σ_3: 15–20 MPa). At confining pressures above 40 MPa, purely compactional deformation was reported and, consequently, decreasing permeability (as expected). This is in agreement with Holt (1990), who showed the same behaviour for another very porous sandstone: the Red Wildmoor (25% porosity).

The difference between these contradicting experimental results in the brittle field cannot be explained satisfactorily. For Morita et al. (1992) it must be remarked that the permeability increase due to dilatancy was very small. Azeemuddin et al. (1995) actually fit their discrete permeability measurements with trendlines, which suggest a permeability increase at higher stresses, but the actual data does not, in the author's opinion, really support this assumption (see Fig. 10B)

Another factor, which is often neglected during triaxial experiments, is the ratio (λ) between pore pressure and confining pressure:

$$\lambda = \sigma_{fl} / \sigma_3 \tag{9}$$

with λ pore-pressure factor, σ_{fl} pore pressure and σ_3 confining pressure.

This ratio reflects the so-called pore-fluid factor (λ_v), which gives the level of fluid pressure at depth z in the Earth's crust and, after Sibson (1992), it is defined as:

$$\lambda_v = P_f / \sigma_v = P_f / (\rho_r g z) \tag{10}$$

with P_f pore fluid pressure at depth z, σ_v minimum stress at depth z, ρ_r average rock density, g gravitational acceleration and z depth.

Natural values for λ range between 0.33 (hydrostatic conditions) and 1 (lithostatic conditions). A value of 0.33 simply comes from the ratio of fluid density (water) and rock density, which can be assumed as being a third. Pore pressures exceeding the hydrostatic level are called overpressurised. Many studies concerned with the influence of triaxial stress on permeability neglect this ratio and use a fixed pore pressure (mostly in the range of only several MPa) without respect to the confining pressure, which, in some experiments, was as high as several hundred MPa (Zhu and Wong 1997). This means that in many studies, the pore-pressure confining pressure ratio is much lower than would be assumed for natural conditions and, thus, the measured permeability values are much lower than they would be in the field. All experiments performed by the author were conducted at a ratio between 0.3–1 in order to simulate natural conditions. From the literature review, especially the experiments in the cataclastic deformation regime (Holt 1990; Zhu and Wong 1997), were done at very low values of λ (0.1–0.02).

For very low-porosity sandstones, some additional results are found in Heiland and Raab (2001) and Keaney et al. (1998):

– For the Flechtinger Bausandstein sandstone from Germany, a linear relation between permeability and volumetric strain has been established (Heiland and Raab 2001).
– After peak strength, a transient permeability peak was observed in low-porosity sandstones, which is associated with the development of a shear band (Keaney et al. 1998; Heiland and Raab 2001).
– In the post-failure region, the permeability of the sample was determined by the properties of the shear band. Because this shear band mostly consists of smeared clays and crushed grains, its transport properties are very low, which results in decreasing permeability under ongoing shear (Keaney et al. 1998).

Conclusions

Figure 24 presents schematic diagrams for the time–stress developments and the stress–permeability relations for the most common experimental procedures (hydrostatic compression, triaxial compression and uniaxial strain conditions). The permeability evolution of high-porosity rock under all these stress paths shows a similar and quite logical feature: with increasing stress the permeability decreases continuously; once the stresses get high enough to initiate pore collapse and grain crushing, permeability reduction undergoes a sharp decline. The only stress condition under which a permeability increase was found are the triaxial compression tests on low-porosity rocks, such as highly compacted sandstones, crystalline rock and even rocksalt (Zoback and Byerlee 1975a; Keaney et al. 1998; Popp et al. 1999; Hunsche and Schulze 2000; Heiland 2002; Heiland and Raab 2001). This permeability increase is a result of brittle rocks in triaxial compression undergo dilatant deformation: that is microcracking causing an increase in pore volume. Dilatant deformation in triaxial compression tests is caused by high shear stresses, which result from the high stress difference between confining pressure and axial stress in this test condition.

For field applications these simple statements are nevertheless important information. In the case of a reservoir (oil, gas or water), production of the fluid will, under most conditions, lead to a stress path that does not produce shear stresses high enough to cause much dilatancy. This means that for most reservoir depletion scenarios a continuously decreasing permeability trend can be assumed.

In the case of underground waste repositories, the situation is the opposite: around deep-seated excavations a zone of high differential stress and, thus, high deformation develops, which causes a considerable increase in rock mass permeability.

References

Al-Harthy SS, Dennis J, Ying XD, Marsden, RJ (1996) Petrophysical properties under true triaxial stress for hydrocarbon recovery prediction. Paper presented at SPE Permian Basin Oil and Gas Recovery Conference in Midland, Texas, 25–27 March 1998. SPE 39770, pp 191–196

Al-Harthy SS, Dennis J, Ying XD, Marsden RJ (1998) Hysteresis, true-triaxial stress-path and pore pressure effects on permeability. Paper presented at SPE/ISRM Eurock 98 conference

Azeemuddin M, Roegiers J-C, Suir P, Zaman M, Kukreti AR (1995) Stress-dependent permeability measurement of rocks in a triaxial cell. In: Tillerson JR, Wawersik WR (eds) Proceedings of the 35th US Symposium on Rock Mechanics, pp 645–650

Brace WF, Walsh JB, Frangos WT (1968) Permeability of granite under high pressure. J Geophys Res 73(6):2225–2236

Bruno MS, Bovberg CA, Nakagawa FM (1991) Anisotropic stress influence on the permeability of weakly-cemented sandstones. In: Roegers J-C (ed) Proceedings of the 32nd US Symposium on Rock Mechanics, p 375–383

David C, Wong T-F, Zhu W, Zhang J (1994) Laboratory measurements of compaction-induced permeability change in porous rock: implications for the generation and maintenance of pore pressure excess in the crust. PAGEOPH 143(1/2/3):425–456

Heiland J (2002) Permeability of triaxially compressed sandstone influence of deformation and strain-rate on permeability. J Pure Appl Geophys (PAGEOPH) (in press)

Heiland J, Raab S (2001) Experimental investigation of the influence of differential stress on permeability of a Lower Permian (Rotliegend) sandstone deformed in the brittle deformation field. Phys Chem Earth 26(1–2):33–38

Holt RM (1990) Permeability reduction induced by a non-hydrostatic stress field. SPE Formation Evaluation, Dec 1990, pp 444–448

Hunsche U, Schulze O (2000) Measurement and calculation of the evolution of dilatancy and permeability in rocksalt. Proceedings of the 3rd Workshop über Kulftaquifere, gekoppelte Prozesse, Hannover, Nov. 2000

Keaney GMJ, Meredith PG, Murrel SAF. (1998) Laboratory study of permeability evolution in a "tight" sandstone under non-hydrostatic stress conditions. Paper presented at the Eurock 96 in Trondheim, SPE/ISRM paper 47265, pp 329–335

Khan M, Teufel LW (2000) The effect of geological and geomechanical parameters on reservoir stress path and is importance in studying permeability anisotropy. SPE Reservoir Eval Eng 3(5):394–400

Kranz RL, Saltzman JS, Blacic JD (1990) Hydraulic diffusivity measurements on laboratory rock samples using an oscillating pore pressure method. Int J Rock Mech Min Sci Geomech Abstr 27(5):345–352

Morita N, Gray KE, Fariz AA Srouji, Jogi PN (1992) Rock-property changes during reservoir compaction. SPE Formation Evaluation, Sept. 1992, pp 197–205

Morrow CA, Bo-Chong Z, Byerlee JD (1984) Effective pressure law for permeability of Westerley Granite under cyclic loading. J Geophys Res 91(B3):3870–3876

Popp T, Schulze O, Kern H (1999) Permeation and development of dilatancy and permeability in rocksalt. Proceedings of the 5th Conference on Mechanical Behaviour of Salt (MECASALT V), Bucharest

Rhett DW, Teufel LW (1992a) Stress path dependence of matrix permeability of North Sea sandstone reservoir rock. In: Tillerson JR, Wawersik WR (eds) Proceedings of the 33rd US Symposium on Rock Mechanics, pp 345–353

Rhett DW, Teufel LW (1992b) Effect of reservoir stress path on compressibility and permeability of sandstones. SPE paper 24756

Ruisten H, Teufel LW, Rhett D (1999) Influence of reservoir stress path on deformation and permeability of weakly cemented sandstone reservoir. SPE Reservoir Eval Eng 2(3):266–272

Schutjens PMTM, de Ruig H (1997) The influence of stress path on compressibility and permeability of an overpressurised reservoir sandstone: some experimental data. Phys Chem Earth 22(1–2):97–103

Sibson RH (1992) Implications of fault-valve behaviour for rupture nucleation and recurrence. Tectonophysics 211:283–293

Stormont JC, Daemen JJK (1992) Laboratory study of gas permeability changes in rocksalt during deformation. Int J Rock Mech Mineral Sci Geomech Abstr 29(4):325–342

Walsh JB, Brace WF (1984) The effect of pressure on porosity and the transport properties of rock. J Geophys Res 89(B11):9425–9431

Wong T-F, David C, Zhu W (1997) The transition form brittle faulting to cataclastic flow in porous sandstones: mechanical deformation. J Geophys Res B 102:3009–3025

Zhu W, Wong T-F (1997) The transition from brittle faulting to cataclastic flow: permeability evolution. J Geophys Res B 102:3027–3041

Zoback MD, Byerlee JD (1975a) Permeability and effective stress. Am Assoc Petrol Geol Bull 59:154–158

Zoback MD, Byerlee JD (1975b) The effect of microcrack dilatancy on the permeability of Westerley Granite. J Geophys Res 80(5):752–755